

M(II)-dipyridylamide-based coordination frameworks (M=Mn, Co, Ni): Structural transformation

Biing-Chiau Tzeng*, TamilSelvi Selvam, Miao-Hsin Tsai

Department of Chemistry and Biochemistry, National Chung Cheng University, 168 University Rd., Min-Hsiung, Chiayi 62102, Taiwan

ARTICLE INFO

Article history:

Received 8 June 2016

Received in revised form

7 August 2016

Accepted 9 August 2016

Available online 9 August 2016

Keywords:

Dipyridylamide

Coordination framework

Structural transformation

Double-zigzag

Polyrotaxane

X-ray diffraction

ABSTRACT

A series of 1-D double-zigzag ($\{[M(\text{papx})_2(\text{H}_2\text{O})_2](\text{ClO}_4)_2\}_n$; M=Mn, x=s (1), x=o (3); M=Co, x=s (4), x=o (5); M=Ni, x=s (6), x=o (7)) and 2-D polyrotaxane ($\{[\text{Mn}(\text{paps})_2(\text{ClO}_4)_2]_n$ (2)) frameworks were synthesized by reactions of $M(\text{ClO}_4)_2$ (M=Mn, Co, and Ni) with papx (paps, N,N'-bis(pyridylcarbonyl)-4,4'-diaminodiphenylthioether; papo, N,N'-bis(pyridylcarbonyl)-4,4'-diaminodiphenyl ether), which have been isolated and structurally characterized by X-ray diffraction. Based on powder X-ray diffraction (PXRD) experiments, heating the double-zigzag frameworks underwent structural transformation to give the respective polyrotaxane ones. Moreover, grinding the solid samples of the respective polyrotaxanes in the presence of moisture also resulted in the total conversion to the original double-zigzag frameworks. In this study, we have successfully extended studies to Mn^{II}, Co^{II}, and Ni^{II} frameworks from the previous Zn^{II}, Cd^{II}, and Cu^{II} ones, and interestingly such structural transformation is able to be proven experimentally by powder and single-crystal X-ray diffraction studies as well.

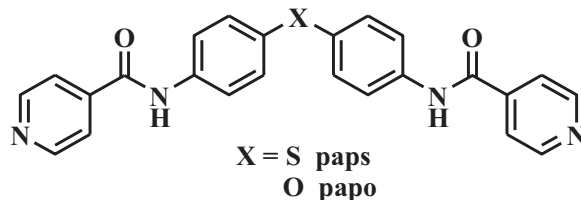
© 2016 Elsevier Inc. All rights reserved.

1. Introduction

There has been continuing and increasing interest in the construction of solid-state architectures and metal-organic frameworks (MOFs) [1] due to their useful applications in chemical sieving, sensing, catalysis, gas sorption, and so on [2]. One of the challenges, which are often encountered in the design and synthesis of such materials, is unpredictability of the solid-state frameworks and their dimensionalities [1,2]. It is noted that the complex formation has been found to be highly dependent on the coordination geometry and number of metal ions, metal/ligand ratios, the flexibility of the ligand backbones, counterions, and solvents in the reaction media [3]. Of these solid-state materials and/or MOFs, so far much attention has been drawn toward flexible and dynamic frameworks, where their structures and properties could be reversibly changed by external stimuli (i.e., heat, vapor, pressure, etc.) [4]. In this regard, the design and synthesis of a host framework with dynamic behavior that can interact with certain guest molecules in a switchable and reversible manner is particularly of interest as a new generation of solid-state materials [5].

Sauvage and co-workers pioneered to build up the research into a new class of metal-containing rotaxanes [6a–c], and thus metal-containing rotaxanes and polyrotaxane networks have been suggested to be the basic elements for constructing various

nanoscale machines and motors in the future [6]. As one exciting branch of the entangled systems polyrotaxane frameworks, where macrocycles such as cyclic polyethers, cyclodextrins, and metal-containing molecular loops threaded into 1-D polymeric chains, have received much attention due to their unusual structural topologies [7]. Robson and co-workers first reported a novel coordination polymer [7a,b], $[\text{Ag}_2(\text{bix})_3(\text{NO}_3)_2]_n$ (bix = 1,4-bis(imidazol-1-ylmethyl)benzene), which consisted of 1-D polymeric chains that were knitted together to generate 2-D polyrotaxane frameworks. In the meantime, Chen and co-workers reported another remarkable polyrotaxane framework of $\text{Cu}_2(\text{bpa})_2(\text{phen})_2(\text{H}_2\text{O})_2$ (bpa = biphenyl-4,4'-dicarboxylate, phen = 1,10-phenanthroline) [8], in which interlocking of the lateral phen ligands of the molecular rhombi of $[\text{Cu}_2(\text{bpa})_2(\text{phen})_2(\text{H}_2\text{O})_2]_2$ led to stacking in the cavities of the adjacent rhombi through intermolecular $\pi \cdots \pi$ interactions in the solid state.



Reversible structural transformation and mechanochromic luminescence of 1-D double-zigzag $\{[\text{Zn}(\text{paps})_2(\text{H}_2\text{O})_2](\text{ClO}_4)_2\}_n$ (paps = N,N'-bis(pyridylcarbonyl)-4,4'-diaminodiphenyl thioether) and 2-D polyrotaxane $[\text{Zn}(\text{paps})_2(\text{ClO}_4)_2]_n$ frameworks [9a,9b] as

* Corresponding author.

well as their respective N,N'-bis(pyridylcarbonyl)-4,4'-diaminodiphenyl ether (papo) analogs have been demonstrated in our previous studies, [9b] where both double-zigzag and polyrotaxane frameworks were synthesized depending on the presence or absence of water in the reaction media, respectively. Significantly, both frameworks can be reversibly interconverted by heating and grinding in the presence of moisture, and such structural transformation is able to be proven experimentally by powder and single-crystal X-ray diffraction studies. We have examined the effects of the Cd^{II} and Cu^{II} on the assembly process [9c,9e] and structural transformation. Herein we extend our studies to the frameworks containing Mn^{II}, Co^{II}, and Ni^{II}, and also investigate their structural transformation behavior.

2. Experimental section

N,N'-bis(pyridylcarbonyl)-4,4'-diaminodiphenyl thioether (paps) and N,N'-bis(pyridylcarbonyl)-4,4'-diaminodiphenyl ether (papo) were prepared following the literature methods [9]. All solvents for syntheses (analytical grade) were used without further purification. Infrared (IR) spectra were recorded with samples in the form of KBr pellets on a Perkin-Elmer PC 16 FTIR spectrometer. The powder X-ray diffraction (PXRD) data were recorded on a Bruker D2 Phaser with $\lambda(\text{Cu K}\alpha) = 1.5418 \text{ \AA}$ and a scan speed of $2^\circ(2\theta)/\text{min}$ as well as a 2θ range of 2° to 60° . Thermal gravimetric analysis (TGA) measurements were performed using a Perkin-Elmer STA6000 thermal analyzer. Elemental analysis (EA) of the complexes was performed on an Elementar vario EL III Heraeus CHNOS Rapid F002 elemental analyzer and the solid samples were pre-treated by subjecting to vacuum overnight.

2.1. Synthesis

$\{[\text{Mn}(\text{paps})_2(\text{H}_2\text{O})_2](\text{ClO}_4)_2\}_n$ (**1**): A solution of $\text{Mn}(\text{ClO}_4)_2 \cdot n\text{H}_2\text{O}$ (15 mg, 0.059 mmol) and paps (15 mg, 0.035 mmol) were dissolved in $\text{MeOH}/\text{CHCl}_3/\text{H}_2\text{O}$ (3 mL/3 mL/0.2 mL), followed by vapor diffusion of diethyl ether. Colorless color crystals were formed with the yield of 55%. FT-IR (KBr): $\nu_{\text{N-H}} = 3230 \text{ cm}^{-1}$, $\nu_{\text{C=O}} = 1661 \text{ cm}^{-1}$ (s), $\nu_{\text{C=C}} = 1591, 1494 \text{ cm}^{-1}$, $\nu_{\text{Cl-O}} = 1108 \text{ cm}^{-1}$ (s). Anal. Calcd (%) for $\text{C}_{48}\text{H}_{40}\text{Cl}_2\text{MnN}_8\text{O}_{14}\text{S}_2$: C 50.45, H 3.53, N 9.80; found: C 50.74, H 3.46, N 9.50.

$\{[\text{Mn}(\text{paps})_2(\text{ClO}_4)_2]\}_n$ (**2**): A solution of $\text{Mn}(\text{ClO}_4)_2 \cdot n\text{H}_2\text{O}$ (15 mg, 0.059 mmol) and paps (15 mg, 0.035 mmol) were dissolved in dry solvents of $\text{MeOH}/\text{CHCl}_3$ (3 mL/3 mL), followed by vapor diffusion of dry diethyl ether under N_2 atmosphere. Colorless crystals were formed with the yield of 42%. FT-IR (KBr): $\nu_{\text{N-H}} = 3229 \text{ cm}^{-1}$, $\nu_{\text{C=O}} = 1655 \text{ cm}^{-1}$, $\nu_{\text{C=C}} = 1588, 1495 \text{ cm}^{-1}$, $\nu_{\text{Cl-O}} = 1114 \text{ cm}^{-1}$. Anal. Calcd (%) for $\text{C}_{48}\text{H}_{36}\text{Cl}_2\text{MnN}_8\text{O}_{12}\text{S}_2$: C 52.09, H 3.28, N 10.12; found: C 52.29, H 3.33, N 9.95.

$\{[\text{Mn}(\text{papo})_2(\text{H}_2\text{O})_2](\text{ClO}_4)_2\}_n$ (**3**): A solution of $\text{Mn}(\text{ClO}_4)_2 \cdot n\text{H}_2\text{O}$ (120 mg, 0.472 mmol) and papo (30 mg, 0.073 mmol) were dissolved in $\text{MeOH}/\text{CHCl}_3/\text{H}_2\text{O}$ (2.5 mL/3.5 mL/0.15 mL), followed by vapor diffusion of diethyl ether. Pale-yellow crystals were formed with the yield of 65%. FT-IR (KBr): $\nu_{\text{N-H}} = 3239 \text{ cm}^{-1}$, $\nu_{\text{C=O}} = 1661 \text{ cm}^{-1}$, $\nu_{\text{C=C}} = 1601 \text{ cm}^{-1}$, $\nu_{\text{Cl-O}} = 1115 \text{ cm}^{-1}$. Anal. Calcd (%) for $\text{C}_{48}\text{H}_{40}\text{Cl}_2\text{MnN}_8\text{O}_{16}$: C 51.90, H 3.63, N 10.09; found: C 51.85, H 3.78, N 9.87.

$\{[\text{Co}(\text{paps})_2(\text{H}_2\text{O})_2](\text{ClO}_4)_2\}_n$ (**4**): paps (10 mg, 0.02 mmol) was dissolved in 6 mL of methanol: chloroform (2:1) mixture and $\text{Co}(\text{ClO}_4)_2 \cdot 6\text{H}_2\text{O}$ (15 mg, 0.04 mmol) was dissolved in 0.3 mL of water. These solutions were mixed together, followed by diffusion of diethyl ether to crystallize pink crystals with the yield of 48%. FT-IR (KBr): $\nu_{\text{N-H}} = 3228 \text{ cm}^{-1}$, $\nu_{\text{C=O}} = 1657 \text{ cm}^{-1}$, $\nu_{\text{C=C}} = 1589, 1494 \text{ cm}^{-1}$, $\nu_{\text{Cl-O}} = 1106 \text{ cm}^{-1}$. Anal. Calcd (%) for $\text{C}_{48}\text{H}_{44}\text{Cl}_2\text{N}_8\text{O}_{16}\text{S}_2\text{Co}$: C 48.74, H 3.75, N 9.47; found: C 48.70, H 4.01, N 9.37.

$\{[\text{Co}(\text{papo})_2(\text{H}_2\text{O})_2](\text{ClO}_4)_2\}_n$ (**5**): papo (10 mg, 0.02 mmol) was dissolved in 6 mL of methanol: chloroform (2:1) mixture and $\text{Co}(\text{ClO}_4)_2 \cdot 6\text{H}_2\text{O}$ (15 mg, 0.04 mmol) dissolved in 0.3 mL of water. These solutions were mixed together, followed by diffusion of diethyl ether to crystallize pink crystals with the yield of 38%. FT-IR (KBr): $\nu_{\text{N-H}} = 3243 \text{ cm}^{-1}$, $\nu_{\text{C=O}} = 1657 \text{ cm}^{-1}$, $\nu_{\text{C=C}} = 1600, 1500 \text{ cm}^{-1}$, $\nu_{\text{Cl-O}} = 1106 \text{ cm}^{-1}$. Anal. Calcd (%) for $\text{C}_{48}\text{H}_{44}\text{Cl}_2\text{N}_8\text{O}_{18}\text{Co}$: C 50.10, H 3.85, N 9.74; found: C 50.06, H 3.86, N 9.65.

$\{[\text{Ni}(\text{paps})_2(\text{H}_2\text{O})_2](\text{ClO}_4)_2\}_n$ (**6**): paps (5 mg, 0.01 mmol) was dissolved in 2 mL of methanol: chloroform mixture and $\text{Ni}(\text{ClO}_4)_2 \cdot 6\text{H}_2\text{O}$ (25 mg, 0.07 mmol) was dissolved in the same solvent mixture. The reaction solution was kept at 60°C for 24 h and the blue crystals were obtained with the yield of 52%. FT-IR (KBr): $\nu_{\text{N-H}} = 3230 \text{ cm}^{-1}$, $\nu_{\text{C=O}} = 1657 \text{ cm}^{-1}$, $\nu_{\text{C=C}} = 1589, 1494 \text{ cm}^{-1}$, $\nu_{\text{Cl-O}} = 1110 \text{ cm}^{-1}$. Anal. Calcd (%) for $\text{C}_{48}\text{H}_{44}\text{Cl}_2\text{N}_8\text{O}_{16}\text{S}_2\text{Ni}$: C 48.75, H 3.75, N 9.48; found: C 48.52, H 3.72, N 9.25.

$\{[\text{Ni}(\text{papo})_2(\text{H}_2\text{O})_2](\text{ClO}_4)_2\}_n$ (**7**): papo (15 mg, 0.04 mmol) was dissolved in 6 mL of methanol: chloroform mixture, and $\text{Ni}(\text{ClO}_4)_2 \cdot 6\text{H}_2\text{O}$ (20 mg, 0.05 mmol) was dissolved in 0.3 mL of water. These solutions were mixed together, followed by diffusion of diethyl ether to give pale-blue crystals with the yield of 68%. FT-IR (KBr): $\nu_{\text{N-H}} = 3243 \text{ cm}^{-1}$, $\nu_{\text{C=O}} = 1658 \text{ cm}^{-1}$, $\nu_{\text{C=C}} = 1600, 1500 \text{ cm}^{-1}$, $\nu_{\text{Cl-O}} = 1120 \text{ cm}^{-1}$. Anal. Calcd (%) for $\text{C}_{48}\text{H}_{44}\text{Cl}_2\text{N}_8\text{O}_{18}\text{Ni}$: C 50.11, H 3.85, N 9.74; found: C 49.86, H 3.95, N 9.87.

2.2. X-ray crystallography

Suitable crystals were mounted on glass capillaries. Data collection was carried out on a Bruker SMART CCD diffractometer with Mo radiation (0.71073 \AA) at $150(2)$ and $293\text{--}295(2) \text{ K}$ for complexes **1**, **2**, **4**, **5** and **3**, **6**, **7**, respectively. A preliminary orientation matrix and unit cell parameters were determined from 3 runs of 15 frames each, each frame corresponding to 0.3° scan in 20 s, followed by spot integration and least-square refinement. Data were measured using an ω scan of 0.3° per frame for 20 s until a complete hemisphere had been collected. Cell parameters were retrieved using SMART [10a] software and refined with SAINT [10b] on all observed reflections. Data reduction was performed with the SAINT software and corrected for Lorentz and Polarization effects. Absorption corrections were applied with the program SADABS [10c]. The structure was solved by direct methods with the SHELXS-97 [10d] program and refined by full-matrix least-squares methods on F^2 with SHELXL-97 [10e]. All non-hydrogen atomic positions were located in difference Fourier maps and refined anisotropically. Hydrogen atoms were constrained to the ideal geometry using an appropriate riding model. Detailed data collection and refinement of coordination frameworks of **1–7** are summarized in Table 1.

3. Results and discussion

In our previous studies [9], we have shown that how the 1-D double zigzag and 2-D polyrotaxane frameworks containing Zn^{II} -papx ($x = \text{s, o}$) can be interconverted by heating and grinding in the presence of moisture. Besides the effect of the heteroatom in the ligand we also extended to study the effect of the metal ions (i.e. Cd^{2+} , Cu^{2+}), which may provide insight in the structural transformation process. In this study, we further synthesized M-papx frameworks, where the 1-D double-zigzag frameworks of $\{[\text{M}(\text{papx})_2(\text{H}_2\text{O})_2](\text{ClO}_4)_2\}_n$ ($\text{M} = \text{Mn, Co, Ni}$; $x = \text{s, o}$) and one polyrotaxane framework of $[\text{Mn}(\text{paps})_2(\text{ClO}_4)_2]$ have been isolated and structurally characterized by single-crystal X-ray diffraction. Although we could not synthesize and characterize all the related polyrotaxane frameworks, we can still compare the PXRD patterns with those of the related analogs. Thus, the structural

Download English Version:

<https://daneshyari.com/en/article/1329400>

Download Persian Version:

<https://daneshyari.com/article/1329400>

[Daneshyari.com](https://daneshyari.com)